Auxiliary-Field Quantum Monte Carlo Simulations of Neutron Matter in Chiral Effective Field Theory

G. Wlazłowski[1,2], J. W. Holt[2], S. Moroz[2], A. Bulgac[2], K. J. Roche[2,3]
[1] *Faculty of Physics, Warsaw University of Technology, Ulica Koszykowa 75, 00-662 Warsaw, Poland*
[2] *Department of Physics, University of Washington, Seattle, WA 98195, USA and*
[3] *Pacific Northwest National Laboratory, Richland, WA 99352, USA*

(Dated: November 6, 2014)

We present variational Monte Carlo calculations of the neutron matter equation of state using chiral nuclear forces. The ground-state wavefunction of neutron matter, containing non-perturbative many-body correlations, is obtained from auxiliary-field quantum Monte Carlo simulations of up to about 340 neutrons interacting on a 10^3 discretized lattice. The evolution Hamiltonian is chosen to be attractive and spin-independent in order to avoid the fermion sign problem and is constructed to best reproduce broad features of the chiral nuclear force. This is facilitated by choosing a lattice spacing of 1.5 fm, corresponding to a momentum-space cutoff of $\Lambda = 414$ MeV/c, a resolution scale at which strongly repulsive features of nuclear two-body forces are suppressed. Differences between the evolution potential and the full chiral nuclear interaction (Entem and Machleidt $\Lambda = 414$ MeV) are then treated perturbatively. Our results for the equation of state are compared to previous quantum Monte Carlo simulations which employed chiral two-body forces at next-to-next-to-leading order (N2LO). In addition we include the effects of three-body forces at N2LO, which provide important repulsion at densities higher than 0.02 fm^{-3}, as well as two-body forces at N3LO.

PACS numbers: 21.65.Cd, 21.30.-x, 21.60.De, 21.60.Ka

arXiv:1403.3753v2 [nucl-th] 5 Nov 2014

Introduction.— Understanding the static and dynamic properties of neutron matter will be key to addressing fundamental questions at the interface of nuclear physics and astrophysics. The structure and evolution of neutron stars, the identification of viable sites for r-process nucleosynthesis, and the interpretation of observed gravitational waveforms from compact binary mergers depend on neutron matter response functions and the equation of state. The nuclear densities relevant in these phenomena range from dilute neutron matter ($\rho \simeq 0.0005\,\mathrm{fm}^{-3}$), governed largely by the universal properties of unitary Fermi systems, to several times nuclear saturation density ($\rho_0 \simeq 0.16\,\mathrm{fm}^{-3}$) found in the core of neutron stars. Due to the large neutron-neutron scattering length, low-density neutron matter is tractable through nonperturbative many-body methods [1–5], while in the vicinity of nuclear matter saturation density, the equation of state can be computed to various degree of accuracy and controlled approximations through a variety of many-body methods [6–16].

Recently, a number of quantum Monte Carlo (QMC) studies [17–19] of neutron matter have employed microscopic nuclear forces derived within the framework of chiral effective field theory (for recent reviews see Refs. [20–22]). These works have focused on chiral two-body interactions at order $(Q/\Lambda_\chi)^3$ (or next-to-next-leading order, N2LO), where Q refers to the low-energy scale set by the pion mass and nuclear momenta, while Λ_χ is the chiral symmetry breaking scale set by, e.g., vector meson masses.

In the present work we introduce a novel approach to study strongly correlated nuclear systems on the lattice employing auxiliary-field quantum Monte Carlo (AFQMC) simulations free of the fermion sign problem. The method enables the simulation of a larger number of particles than alternative Monte Carlo implementations, and it offers an avenue to extend ab-initio many-body methods into the medium-mass region of the nuclear chart. As an initial application of the method, we focus on the equation of state of cold neutron matter at low to intermediate densities computed from chiral two-body forces at N3LO together with the chiral three-neutron force at N2LO.

The auxiliary-field quantum Monte Carlo simulations are performed free of the fermion sign problem by constructing an attractive, spin-independent effective Hamiltonian inspired by one-boson exchange models. The extent to which such a potential approximates the qualitative features of realistic chiral nuclear forces depends, in part, on the resolution scale at which the nuclear force is constructed. Lowering the resolution scale weakens the short-distance repulsion in the nucleon-nucleon (NN) interaction [23–25], thereby enhancing the role of correlations in the neutron matter ground state that can be generated by such evolution Hamiltonians. In contradistinction with Green Function Monte Carlo simulations [1–3] employing Argonne nuclear potentials where the short-range correlations have an important role, in the present approach the emphasis is on the long-range correlations.

Specifically, we consider the chiral nuclear interaction described in Refs. [11, 26, 27] with the regulating function

$$f(p,p') = \exp[-(p/\Lambda)^{2n} - (p'/\Lambda)^{2n}], \qquad (1)$$

where $n = 10$ and $\Lambda = 414\,\mathrm{MeV/c}$. The value of n is chosen to be large for consistency with the sharp lattice

momentum cutoff. This high-precision nuclear potential reproduces nucleon-nucleon elastic scattering phase shifts up to lab energies of 200 MeV with $\chi^2/\mathrm{DOF} = 1.44$ [28], the properties of the deuteron, the binding energy and lifetime of ^{3}H (with the inclusion of two-body weak currents), as well as the empirical nuclear matter saturation point and critical point of the liquid-gas phase transition [29]. In comparison the optimized evolution potential, expressed as a sum of attractive and repulsive Yukawa interactions, is constrained by NN phase shifts as well as the perturbative equation of state employing the full chiral nuclear potential. The interacting ground state is then obtained from this Hamiltonian by propagating a trial Slater-determinant wavefunction in imaginary time using standard auxiliary-field quantum Monte Carlo techniques [30, 31]. The expectation value of the full chiral Hamiltonian in the evolved ground state on the one hand gives an upper bound on the equation of state and on the other hand can be interpreted as the first-order perturbative correction in powers of the difference between the full chiral interaction and the evolution potential. The present approach establishes the framework for future work directed toward accessing nucleon spectral properties, linear response and various transport properties of dilute neutron matter, similar to what has been demonstrated in the case of the unitary Fermi gas [32–36]. Spin response and neutrino scattering and emissivity [37, 38] as well as collective modes in dilute neutron matter [39] are examples of neutron star and supernova properties that can be addressed.

Auxiliary-field quantum Monte Carlo simulations on the lattice.— Quantum Monte Carlo approaches rely on the very simple idea of projecting out the ground state ψ of a many-body system with Hamiltonian $\hat{H}$ by means of imaginary time evolution $\exp(-\tau\hat{H})\psi_0 \stackrel{\tau\to\infty}{\longrightarrow} \psi$, where ψ_0 is an arbitrary initial state with non-vanishing overlap with the ground state. In practical realizations the projection is performed by successive application of the evolution operator for small imaginary time steps: $\psi(\tau+\Delta\tau) = \exp(-\Delta\tau\,\hat{H})\psi(\tau)$. This short evolution in imaginary time is converted into integral form, and the emerging multidimensional integration is performed by means of Monte Carlo techniques. For fermionic systems one has to introduce a prescription for avoiding the sign problem. The most popular approaches are the "fixed-node" and "fixed phase" approximations [40, 41], where the first one results in a variational approximation to the energy. In this paper we utilize a different strategy to deal with the sign problem for a large class of systems, which by construction also results in a variational estimate of the energy.

Our aim is to compute the ground state energy of the Hamiltonian $\hat{H} = \hat{T} + \hat{V}$, where $\hat{T}$ is kinetic energy operator and $\hat{V} = \hat{V}_{2N} + \hat{V}_{3N} + \cdots$ is the sum of two- and many-body forces. In the following we present calculations including chiral 2N interactions up to order N3LO in addition to the 3N interaction at order N2LO: $\hat{V} = \hat{V}_{2N}^{(\mathrm{N3LO})} + \hat{V}_{3N}^{(\mathrm{N2LO})}$. We work with a low-momentum chiral potential with cutoff parameter $\Lambda = 414\,\mathrm{MeV/c}$ and a steep regulator function [27]. Since the imaginary time evolution of a wavefunction with the full chiral Hamiltonian results in a severe sign problem, we rewrite the Hamiltonian as

$$\hat{H} = (\hat{T} + \hat{V}_{\mathrm{ev}}) + (\hat{V} - \hat{V}_{\mathrm{ev}}) \equiv \hat{H}_{\mathrm{ev}} + \delta\hat{V}, \qquad (2)$$

where we assume that $\hat{H}_{\mathrm{ev}}$ represents a nonperturbative problem that can be solved by means of QMC without the sign problem. By construction we assume that δV can be regarded as a small correction to the energy that can be estimated in perturbation theory. To leading order we find

$$E \lesssim \left\langle \psi \left| \hat{H} \right| \psi \right\rangle = \left\langle \psi \left| \hat{H}_{\mathrm{ev}} \right| \psi \right\rangle + \left\langle \psi \left| \delta\hat{V} \right| \psi \right\rangle, \qquad (3)$$

and $\psi(\tau \to \infty) \sim \exp(-\tau\hat{H}_{\mathrm{ev}})\psi_0$ is the normalized ground state wavefunction of the evolution Hamiltonian. It is clear that our approach provides an upper bound for the ground state energy E of the chiral Hamiltonian.

To construct the evolution Hamiltonian we note that each interaction that is spin-independent and attractive in momentum space ($V_{\mathrm{ev}}(q) \leqslant 0$) leads to a QMC simulation free from the sign problem (see for example [30]). Inspired by the one-boson exchange model, we express the evolution potential as (including the pion):

$$V_{\mathrm{ev}}(q) = \sum_{\alpha=\pi,\sigma,\omega} \frac{V_\alpha}{m_\alpha^2 c^2 + q^2} f(q), \qquad (4)$$

and we apply a regulator function of the form $f(q) = \exp[-(q/\Lambda)^{30}]$. These coupling constants and masses are fit (under the constraint that the sum is not positive) to minimize the expression

$$\begin{aligned}\chi^2 \;=\; & \sum_{i,j} w^{(j)} \left[\delta_{\mathrm{EFT}}^{(j)}(E_i) - \delta_{\mathrm{ev}}^{(j)}(E_i)\right]^2 \\ & + \alpha \left[E_{\mathrm{EFT}}^{(\mathrm{pert.})} - E_{\mathrm{ev}}^{(\mathrm{pert.})}\right]^2 \end{aligned} \qquad (5)$$

where $\delta^{(j)}(E_i)$ are phase shifts for partial waves $j = {}^1S_0, {}^3P_0, {}^3P_1, {}^3P_2$ obtained both for the chiral N3LO and the evolution potentials at given energy E_i, and the weights $w^{(j)}$ are respectively $1, \frac{1}{9}, \frac{3}{9}, \frac{5}{9}$. Thus the P-waves are weighted according their degeneracy. The range of phase shifts included in the fitting procedure is density dependent and contains lab energies from 0 to $\min[6E_{\mathrm{lab}}(k_F), 350]\,\mathrm{MeV}$ where $E_{\mathrm{lab}}(k_F) = 2k_F^2/M$ and k_F is the Fermi momentum. A somewhat similar approach to handle the fermion sign problem was advocated in Ref. [42].

The role of the last term in Eq. (5) is to ensure that the total energy of the neutron system interacting with the evolution potential and computed from second-order

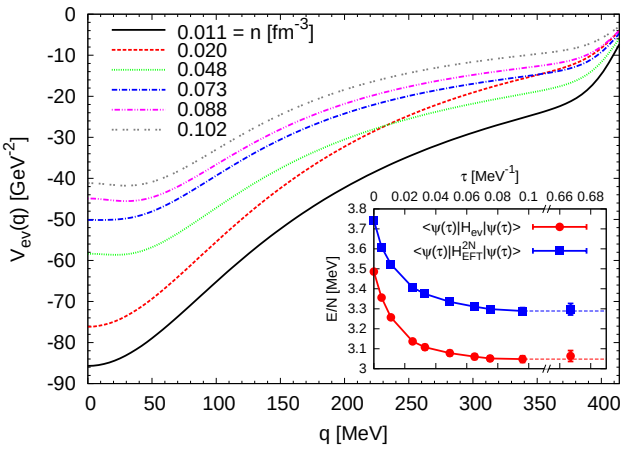

FIG. 1: (Color online) Momentum-space evolution potentials (see Eq. (4)) employed in the imaginary-time propagation of the trial wavefunction, corresponding to different densities. In the inset is shown the expectation values of the evolution potential (red solid circles) and the two-body chiral potential (blue squares) computed for the density $n = 0.011\,\mathrm{fm}^{-3}$.

perturbation theory $E_{\rm ev}^{(\rm pert.)}$ is the same as the energy computed with the chiral potential $E_{\rm EFT}^{(\rm pert.)}$ in the same framework. The "stiffness" of this requirement is governed by the parameter α, and in practice we choose it so that differences in the perturbative estimates of the energy differ by less that 1%. We note also that this kind of evolution Hamiltonian is not necessarily unique, as described in the *Results* section below.

Note that by construction the emerging evolution potential is density dependent, as in the case of the in-medium similarity renormalization group approach [43]. Intuitively, it can be treated as an effective, in-medium two-body interaction, where the density dependence accounts for repulsive effects of nuclear three-body forces, Pauli blocking in the medium, etc. In the zero-density limit the second term of Eq. (5) is negligible and the potential is fitted to phase shifts only and it reproduces correctly low energy scattering parameters, like scattering length or effective range.

Once the evolution potential is constructed, we generate the corresponding many-body wavefunction by means of AFQMC simulations. We consider a set of N neutrons interacting on a three-dimensional cubic spatial lattice of extent $L = N_x l$ and impose periodic boundary conditions. The lattice spacing $l = 1.5\,\mathrm{fm}$ provides a natural ultraviolet cutoff scale, which we impose to be spherical in momentum space and consistent with the cutoff scale of the chiral theory, i.e. $\Lambda = p_{\rm cut} = \pi\hbar/l = 414\,\mathrm{MeV/c}$. The imaginary-time evolution operator $\exp[-\tau\hat{H}_{\rm ev}]$ is expanded using a Trotter-Suzuki decomposition with temporal lattice spacing $\Delta\tau$, and the interaction $V_{\rm ev}$ is represented by means of a continuous Hubbard-Stratonovich (HS) transformation. In order to get faster convergence in the Monte-Carlo evaluation, we approximate the Gaussian quadrature emerging from the HS decomposition by a 5-points quadrature formula, which introduces an error that is small compared to that originating from the Suzuki-Trotter formula. The statistical error for Monte-Carlo quadrature estimation is below 1%.

In this paper we work with lattice size $N_x = 10$, which in previous studies of the unitary Fermi gas [31, 33] led to systematic errors on the order of at most $\sim 10\%$. The main contribution to this error came from high momenta states beyond the momentum cut-off due to the slow decay of the universal high momentum tail in the occupation probability $n(p) \sim p^{-4}$. In the present work with chiral nuclear forces, the momentum distribution exhibits an exponential falloff (see *Results* section below), and therefore we expect improved finite-volume systematic errors. We have developed a new parallel code for these analyses and checked that calculations performed at zero temperature reproduce with sufficient accuracy the zero-temperature Bertsch parameter of the unitary Fermi gas. In particular, the superfluid gap of the unitary Fermi gas and the related properties are accurately reproduced. We consider densities from $0.01\,\mathrm{fm}^{-3}$ to $0.10\,\mathrm{fm}^{-3}$, corresponding to particle numbers ranging from 38 to 342, thus larger than any previous calculations of neutron matter. In order to reduce the discretization errors, we work only with particle numbers corresponding to closed shells in the free Fermi gas model on the lattice. Moreover, we have demonstrated the feasibility of exploring the nonperturbative properties of dilute neutron matter. We performed simulations with 38 particles in 12^3, 14^3 and 16^3 boxes while keeping the lattice spacing fixed at $1.5\,\mathrm{fm}^{-3}$, which correspond to densities 0.0065, 0.0041 and $0.0028, \mathrm{fm}^{-3}$ respectively.

In addition to discretization errors and statistical errors (below 1%), our approach introduces another source of error, related to the fact that we approximate the ground-state wavefunction of the chiral Hamiltonian by the ground-state of the evolution Hamiltonian. The best strategy to quantify this error is to calculate the second-order correction in Eq. (3). In this paper we show only that the first-order correction is small (at most 10%) and comparable to discretization errors. Assuming the perturbativeness of the expansion in Eq. (3) we conclude that discretization errors are dominant in our approach, however, strict quantification will be subject of future studies.

Results.— In Fig. 1 we plot the evolution potentials as a function of the momentum transfer q for different densities obtained by minimizing the χ^2 function in Eq. (5). Different initial choices for the coupling strengths and masses of the "σ" and "ω" mesons resulted in nearly identical evolution potentials, except at the largest densities where variations in the starting values gave a 2% spread in the final energy per particle. We observe that the imposed energy constraint leads to a decrease in the

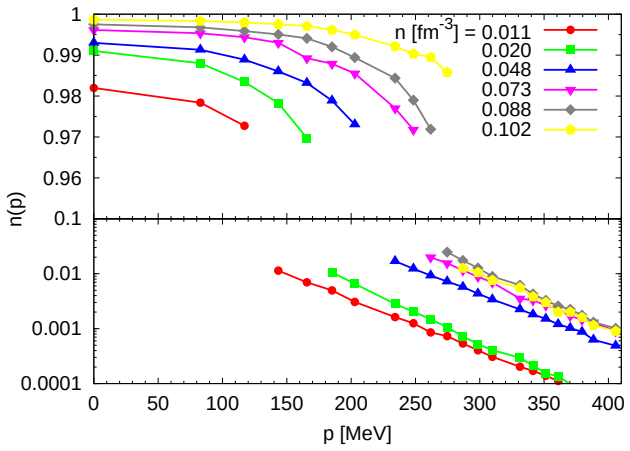

FIG. 2: (Color online) Occupation probabilities of neutron matter as a function of momentum for selected densities.

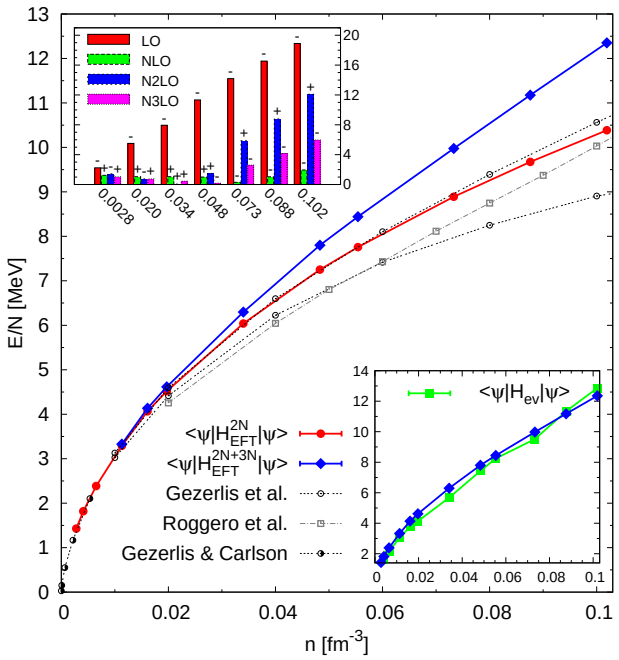

FIG. 3: (Color online) Equation of state of pure neutron matter calculated using AFQMC with the N3LO chiral two-nucleon potential (red circles) plus the N2LO three-nucleon contribution (blue diamonds). For comparison we show the results of Gezerlis *et al.* [18], Roggero *et al.* [19] and Gezerlis & Carlson [44] of QMC calculations with two-body forces alone. In the upper inset we show the contributions to the energy per particle from different orders in the chiral expansion ("+" and "−" refer to repulsive and attractive components, respectively). The lower inset demonstrates that the last term in Eq. (3) is perturbative.

overall strength of the evolution potentials as the density is increased. Physically this accounts for the presence of repulsive two- and three-body forces that become more important as the density increases, so on average the total strength of the attractive nuclear potential must be reduced.

As an initial trial wavefunction we consider the Slater determinant of the lowest N occupied discrete plane wave orbitals. The expectation values of the evolution Hamiltonian and the chiral nuclear potential at imaginary time $\tau = 0$ are then simply the lattice Hartree-Fock energies. Deviations between the continuum Hartree-Fock predictions and those of the lattice were found to be at most a few percent when the particle number corresponds to closed shells in the free Fermi gas model on the lattice. In the inset of Fig. 1 we show the evolution in imaginary time of $\langle\psi(\tau)|\hat{H}_{\rm ev}|\psi(\tau)\rangle$ and $\langle\psi(\tau)|\hat{H}^{\rm 2N}_{\rm EFT}|\psi(\tau)\rangle$ for density $n = 0.011\,{\rm fm}^{-3}$. Note that the left- and right-hand wavefunctions are evolved separately. Typically we observe a very good convergence for imaginary times about $\tau \approx 0.1\,{\rm MeV}^{-1}$, which requires about 300 imaginary time steps. Apart from a nearly constant shift, the imaginary-time dependence for both expectation values is very similar, indicating that our fitting procedure indeed produces the evolution potential, which correctly captures global features of the chiral potential.

Our calculation procedure gives us access to the wave function in both the coordinate and momentum representation. In Fig. 2 we show the momentum distribution associated with the evolution Hamiltonian $\hat{H}_{\rm ev}$ for pure neutron matter at selected densities. As the density increases and the evolution Hamiltonian weakens, the depletion in the occupation probability at low momenta is reduced. In all simulations the single-particle occupation probabilities for the highest energy states is below one percent.

In Fig. 3 we present AFQMC results for the equation of state of pure neutron matter [45]. Evaluating only the chiral two-nucleon force in the correlated ground state (shown in red solid circles), we find that the equation of state is consistent with previous quantum Monte Carlo simulations employing N2LO chiral 2N interactions [18, 19]. At very low densities our results match perfectly onto the QMC results obtained with the effective interaction which captures correctly only scattering length and effective range [44]. At these low densities the pairing correlations are very strong ($\Delta/\varepsilon_F \approx 1/4$, where ε_F is the Fermi energy of a free neutron gas with the same density) and the nice agreement with [44] demonstrates that we capture them very accurately. The chiral nuclear potential most similar the one employed in the current study is the local 400 MeV cutoff potential of Ref. [18] (see the lower line of gray open circles in Fig. 3). Our results for the energy per particle are more repulsive by about 1 MeV, and although further investigations are required, we note that the chiral nuclear interaction in Ref. [18] is more strongly attractive in relative P-waves than the potential we employ. Computing also the expectation value of the N2LO three-nucleon force over the

evolved wavefunction introduces significant additional repulsion above $n = 0.02\,\mathrm{fm}^{-3}$, as seen from the solid blue diamonds in Fig. 3. Differences between the expectation value of the evolution Hamiltonian and the full chiral nuclear 2N + 3N interaction (which can be regarded as the first-order correction to the energy in perturbation theory) are small as shown in the lower-right inset to Fig. 3. In the upper-left inset, we show the expectation value of the chiral Hamiltonian decomposed according to the chiral order.

In the above calculations we translate the lattice results to the continuum limit with the following procedure: i) from the lattice simulations we extract the dimensionless quantity $\frac{\langle\psi|\hat{O}|\psi\rangle}{\langle\psi_0|\hat{O}|\psi_0\rangle}$, where ψ is the ground state of the evolution Hamiltonian, ψ_0 is the free Fermi gas wave function, and both expectation values are computed on the lattice, ii) to convert the lattice result into a dimensionful quantity we multiply by $\langle\psi_0|\hat{O}|\psi_0\rangle^{(\mathrm{cont.})}$, computed in the continuum limit.

Acknowledgments.— We are grateful to P. Magierski and R. Machleidt for helpful discussion, and we thank A. Gezerlis and A. Roggero for sharing the results of their numerical simulations. This work was supported in part by US DOE Grant No. DE-FG02-97ER-41014 and the Polish National Science Center (NCN) under Contracts No. UMO-2013/08/A/ST3/00708 and No. UMO-2012/07/B/ST2/03907. Calculations reported here have been performed at the University of Washington Hyak cluster funded by the NSF MRI Grant No. PHY-0922770 and at the Interdisciplinary Centre for Mathematical and Computational Modelling (ICM) at University of Warsaw. G.W. acknowledges the Center for Advanced Studies at Warsaw University of Technology for the support under Contract No. 58/2013 (international research scholarships financed by the European Union from the European Social Funds, CAS/32/POKL). KJR was supported by the DOE Office of Science, Advanced Scientific Computing Research, under award number 58202 "Software Effectiveness Metrics" (Lucille T. Nowell).

[1] S. Gandolfi, A. Y. Illarionov, F. Pederiva, K. E. Schmidt, and S. Fantoni, Phys. Rev. C **80**, 045802 (2009).
[2] S. Gandolfi, A. Y. Illarionov, K. E. Schmidt, F. Pederiva, and S. Fantoni, Phys. Rev. C **79**, 054005 (2009).
[3] A. Gezerlis and J. Carlson, Phys. Rev. C **81**, 025803 (2010).
[4] G. Wlazłowski and P. Magierski, Phys. Rev. C **83**, 012801(R) (2011).
[5] G. Hagen, T. Papenbrock, A. Ekström, K. A. Wendt, G. Baardsen, S. Gandolfi, M. Hjorth-Jensen, and C. J. Horowitz, Phys. Rev. C **89**, 014319 (2014).
[6] K. Hebeler and A. Schwenk, Phys. Rev. C **82**, 014314 (2010).
[7] A. Lovato, O. Benhar, S. Fantoni, and K. E. Schmidt, Phys. Rev. C **85**, 024003 (2012).
[8] M. Baldo, A. Polls, A. Rios, H.-J. Schulze, and I. Vidaña, Phys. Rev. C **86**, 064001 (2012).
[9] A. Rios and V. Somà, Phys. Rev. Lett. **108**, 012501 (2012).
[10] A. Carbone, A. Polls, and A. Rios, Phys. Rev. C **88**, 044302 (2013).
[11] L. Coraggio, J. W. Holt, N. Itaco, R. Machleidt, and F. Sammarruca, Phys. Rev. C **87**, 014322 (2013).
[12] J. W. Holt, N. Kaiser, and W. Weise, Phys. Rev. C **87**, 014338 (2013).
[13] A. Ekström, G. Baardsen, C. Forssén, G. Hagen, M. Hjorth-Jensen, G. R. Jansen, R. Machleidt, W. Nazarewicz, T. Papenbrock, J. Sarich, et al., Phys. Rev. Lett. **110**, 192502 (2013).
[14] G. Baardsen, A. Ekström, G. Hagen, and M. Hjorth-Jensen, Phys. Rev. C **88**, 054312 (2013).
[15] I. Tews, T. Krüger, K. Hebeler, and A. Schwenk, Phys. Rev. Lett. **110**, 032504 (2013).
[16] T. Krüger, I. Tews, K. Hebeler, and A. Schwenk, Phys. Rev. C **88**, 025802 (2013).
[17] E. Epelbaum, H. Krebs, D. Lee, and U. G. Meißner, Eur. Phys. J. A **40**, 199 (2009).
[18] A. Gezerlis, I. Tews, E. Epelbaum, S. Gandolfi, K. Hebeler, A. Nogga, and A. Schwenk, Phys. Rev. Lett. **111**, 032501 (2013).
[19] A. Roggero, A. Mukherjee, and F. Pederiva, Phys. Rev. Lett. **112**, 221103 (2014).
[20] E. Epelbaum, H.-W. Hammer, and U.-G. Meissner, Rev. Mod. Phys. **81**, 1773 (2009).
[21] R. Machleidt and D. R. Entem, Phys. Rept. **503**, 1 (2011).
[22] J. W. Holt, N. Kaiser, and W. Weise, Prog. Part. Nucl. Phys. **73**, 35 (2013).
[23] S. K. Bogner, T. T. S. Kuo, and A. Schwenk, Phys. Rep. **386**, 1 (2003).
[24] S. K. Bogner, R. J. Furnstahl, and A. Schwenk, Prog. Part. Nucl. Phys. **65**, 94 (2010).
[25] K. A. Wendt, R. J. Furnstahl, and S. Ramanan, Phys. Rev. C **86**, 014003 (2012).
[26] L. Coraggio, A. Covello, A. Gargano, N. Itaco, D. R. Entem, T. T. S. Kuo, and R. Machleidt, Phys. Rev. C **75**, 024311 (2007).
[27] L. Coraggio, J. W. Holt, N. Itaco, R. Machleidt, L. E. Marcucci, and F. Sammarruca, Phys. Rev. C **89**, 044321 (2014).
[28] R. Machleidt (private communication).
[29] C. Wellenhofer, J. W. Holt, N. Kaiser, and W. Weise, Phys. Rev. C **89**, 064009 (2014).
[30] S. E. Koonin, D. J. Dean, and K. Langanke, Phys. Rept. **278**, 1 (1997).
[31] A. Bulgac, J. E. Drut, and P. Magierski, Phys. Rev. A **78**, 023625 (2008).
[32] G. Wlazłowski, P. Magierski, A. Bulgac, and K. J. Roche, Phys. Rev. A **88**, 013639 (2013).
[33] G. Wlazłowski, P. Magierski, J. E. Drut, A. Bulgac, and K. J. Roche, Phys. Rev. Lett. **110**, 090401 (2013).
[34] G. Wlazłowski, P. Magierski, and J. E. Drut, Phys. Rev. Lett. **109**, 020406 (2012).
[35] P. Magierski, G. Wlazłowski, and A. Bulgac, Phys. Rev. Lett. **107**, 145304 (2011).
[36] P. Magierski, G. Wlazłowski, A. Bulgac, and J. E. Drut, Phys. Rev. Lett. **103**, 210403 (2009).
[37] G. Shen, S. Gandolfi, S. Reddy, and J. Carlson, Phys.

Rev. C **87**, 025802 (2013).
[38] G. Shen and S. Reddy, Phys. Rev. C **89**, 032802(R) (2014).
[39] N. Chamel, D. Page, and S. Reddy, Phys. Rev. C **87**, 035803 (2013).
[40] J. Carlson, J. E. Gubernatis, G. Ortiz, and S. Zhang, Phys. Rev. B **59**, 12788 (1999).
[41] G. Ortiz, D. M. Ceperley, and R. M. Martin, Phys. Rev. Lett. **71**, 2777 (1993).
[42] J. E. Lynn and K. E. Schmidt, Phys. Rev. C **86**, 014324 (2012).
[43] K. Tsukiyama, S. K. Bogner, and A. Schwenk, Phys. Rev. Lett. **106**, 222502 (2011).
[44] A. Gezerlis and J. Carlson, Phys. Rev. C **77**, 032801(R) (2008).
[45] For a table of the energy per particle as a function of density, see online supplemental material.